Collective radial expansion in Au+Au reactions from 0.25 to 2 GeV/nucleon

Frank Daffin,* Kevin Haglin, and Wolfgang Bauer
National Superconducting Cyclotron Laboratory, Michigan State University, East Lansing, Michigan 48824-1321
(Received 13 May 1996)

A nonthermal expansive component has recently been interpreted from the observed light fragment spectra in Au + Au collisions. We have used the BUU transport model to generate several different freezeout surfaces and applied a coalescence algorithm to approximate the complete final state. We vary the microscopic details leading to specific equations of state, reduce cross sections, and isolate the effect of compression on the spectra for protons and helium isotopes. We find a radial flow signal consistent with experiment in the energy range 0.25*A* to 1.15*A* GeV, but find it to be rather insensitive to the microscopic details of the model calculations. [S0556-2813(96)02609-X]

PACS number(s): 25.75.Ld, 24.10.Jv, 24.10.Nz, 24.10.Pa

I. INTRODUCTION

The expansion of hot, excited nuclear matter formed in the collision of heavy ions is governed by an interplay between mean field interaction, nucleon-nucleon scattering, and the Coulomb force. In an effort to understand the effects of these forces, we have turned to the study of these collisions through observables sensitive to the dynamics they govern. Observables such as collective flow phenomena [1–8], azimuthal anisotropies [5,9], and others [10] have been used in the past. Flow originates when nuclear matter from nucleus-nucleus collisions attains a strongly correlated momentum distribution principally through effective strong interactions.

Of the models used to study heavy ion collisions at intermediate energies, the BUU model [11–13] is among the most fruitful. The model propagates nucleons with Hamilton's equations through the influence of experimentally observed nucleon-nucleon cross sections, the Coulomb field and a nuclear mean field which is dependent upon local nucleon density or both local nucleon density and the local momentum distribution [14]. However, BUU evolves the single-particle phase-space distribution and there is no provision in the nuclear mean field for higher order correlations. The result is a numerical model that is successful at predicting and providing insight into single-particle observables [2,4,5], but at the same time not suited to providing the same for clustering and fragmentation.

With its success in predicting and reproducing empirical transverse, in-plane proton momentum distributions [4,5], one may naturally ask whether BUU can generate the radial flow recently interpreted from central Au + Au collisions [8]. In that study, the EOS-TPC Collaboration focused on low rapidity yields of protons, deuterons, tritons, ^{3}He, and alpha fragments as functions of kinetic energy. They analyzed the spectra with a radially expanding thermal model [15] from which approximate temperatures and global radial flow velocities for the collision volume were extracted.

We use a coalescence model to convert the single-particle phase-space distribution evolved in BUU to freezeout into a final-state distribution of free protons, deuterons, tritons, ^{3}He, and alpha particles. Then, using χ^2/ν minimization, we fit the resulting spectra to thermal yet radially expanding distributions to assign a common temperature and expansion velocity for the collision volume.

Section II contains a discussion of the hybrid model used to generate the nucleon phase-space distribution, convert it to distributions of light fragments, and finally to extract the temperature and radial flow velocities of the participant volumes. Section III is a presentation of our results and a comparison to experimental data, and our conclusions are presented in Sec. IV.

II. MODELS AND CALCULATIONS

The BUU transport equation evolves in time a single-nucleon phase-space distribution under the influences of nucleon-nucleon collisions, the Coulomb field, and a nuclear mean field. The nuclear mean field is [17]

$$U=A\left(\frac{\rho}{\rho_0}\right)+B\left(\frac{\rho}{\rho_0}\right)^{\sigma}+\frac{C}{\rho_0}\left\{\int\frac{f(\vec{r},\vec{p}\,')d\vec{p}\,'}{1+[(\vec{p}-\langle\vec{p}\,'\rangle)/\Lambda]^2}+\frac{\rho}{1+[(\vec{p}-\langle\vec{p}\rangle)/\Lambda]^2}\right\}, \tag{2.1}$$

where $\langle\vec{p}\rangle$ is the average local momentum, can be modeled with various combinations of force parameters leading to different compressibilities in addition to toggling the momentum dependence. Values for the parameters in Eq. (2.1) are shown in Table I. The nucleon-nucleon cross sections are

TABLE I. The constants in used in the nuclear mean field. Note that ''soft'' refers to a compressibility K of 215 MeV and ''stiff'' refers to a compressibility of 380 MeV.

EOS	A	B	σ	C	Λ	ρ_0
Soft	−0.109	0.082	7/6	0	−	0.168
Stiff	−0.062	0.03525	2	0	−	0.168
Soft $\vec{p}$	−0.109	0.082	7/6	−0.065	0.416	0.168
Stiff $\vec{p}$	−0.062	0.03525	2	−0.065	0.416	0.168

*Electronic address: daffin@nscl.msu.edu

parametrization from the Particle Data Group with medium modification implemented according to the density dependent prescription:

$$\sigma_{nn}=\sigma_{nn}^{\text{free}}\left(1+\alpha\frac{\rho}{\rho_0}\right), \tag{2.2}$$

where α is varied between -1 and 0, ρ_0 is normal nuclear matter density, and where ρ is the nuclear matter density in the neighborhood of the collision [18,19].

The BUU formalism was used to model Au + Au collisions at energies 0.25, 0.60, 1.0, 1.5, and 2.0 GeV/nucleon with impact-parameter-averaging $b\leqslant 3$ fm, and a hard (compressibility $K=380$ MeV) momentum-dependent nuclear mean field. The nucleons scattered with $\alpha=0$ and the system was evolved until the collision rate dropped to less than one collision per ensemble per time step. It is at this point that the reaction dynamics responsible for clustering and interactions between the clusters becomes important. We matched the experimental acceptance of $\theta_{\text{c.m.}}=90^\circ\pm 15^\circ$ relative to the beam axis, which was chosen to better isolate the anticipated radial flow from directed flow.

Since the EOS-TPC Collaboration focused its attention on the spectra of light fragments in addition to that of free protons, and since our BUU has no self-consistent provision for the production of light fragments, a coalescence algorithm was needed to convert the phase-space distribution of protons and neutrons from the BUU calculations at freezeout into final-state protons, deuterons, tritons, ^{3}He, and alpha particles. Deuterons were formed whenever a proton and a neutron were within a critical radius in configuration space and the same proton and neutron were within a critical radius in momentum space. These critical radii were fixed by minimizing the difference between the final-state proton spectra from the BUU calculation and that from the EOS-TPC study at 1 GeV/nucleon. We found $\Delta R_{\text{deuteron}}=1.5$ fm and $\Delta P=100$ MeV/c. The critical radius in configuration space for heavier fragments was simply increased according to $R_i \propto A_i^{1/3}$ where i is the fragment species, while the critical radius in momentum space was maintained at 100 MeV/c. These values are of the same order of magnitude as length and momentum parameters used in other coalescence models [20,21].

This prescription for coalescence is not original [22,23], though it represents something of a departure from what is more common at these energies: a momentum-space coalescence [24–29]. The success of momentum-space coalescence at intermediate energies is well documented [30–32,21,33,34]. The additional constraint ΔR allows one to explore coalescence simulations where the source size exceeds that of the fragments emitted [35,36]. However, source sizes at energies ~ 1 GeV/nucleon are expected to be of the same order as the fragments emitted from them, effectively negating the need for a constraint in configuration-space [34]. Indeed, in our work to fix the coalescence parameters, we found the spectra to have small sensitivity to changes in ΔR.

The coalescence model used here produces light fragments, all at the same time coordinate, propagates them to infinity free of mutual interaction or interaction with the spectator system, and without the possibility of decay from excited states to ground states. This is tantamount to making nonrelativistic and sudden approximations, in addition to assuming chemical equilibrium is reached for all the fragments, regardless of species, at the same time. It is free, however, of making assumptions about thermal equilibrium, local or otherwise, light fragment potentials and source sizes. The sudden approximation is probably a good one [25] and is used extensively in the older models. All this has the advantage of being relatively simple to code and minimizes the combinatorial burden. There are more sophisticated coalescence models [26,37,38] which are less cavalier in their presumptions about the conditions under which fragmentation, coalescence, and clustering occur. And the imposition of a coalescence ''after-burner'' upon the phase-space distribution evolved using transport codes barren of strong multiparticle interaction fails to answer questions regarding the role of clustering before freezeout, though alternatives do exist [39,40].

The spectra of protons, deuterons, tritons, ^{3}He, and alphas were analyzed using a radially expanding thermal model [15]. In this model the fragments are assumed to possess a thermal velocity distribution characterized by a temperature in Maxwell-Boltzmann statistics, and an overall radial velocity. In the global rest frame the resultant distribution is

$$\frac{d^3N}{dp^3}\sim\exp(-\gamma E/T)\left[\left(\frac{\gamma+T}{E}\right)\frac{\sinh(\lambda)}{\lambda}-\frac{T}{E}\cosh(\lambda)\right], \tag{2.3}$$

where $\gamma\equiv 1/\sqrt{1-\beta^2}$, $\lambda\equiv\gamma\beta p/T$, T is temperature and $\beta\equiv v/c$ is the radial flow velocity. The spectra were fit to Eq. (2.3) by fixing the overall normalization and varying T and β to obtain a minimum χ^2/ν. Global fits constituted simultaneous fits to deuterons, ^{3}He, tritons, and alphas since the proton spectrum was used to fix the critical radii for coalescence.

In addition to the impact-parameter averaged study, we made calculations probing the relative importance of the various features the BUU transport model in terms of their effect on radial flow velocity and temperature. Calculations were again of Au + Au but restricted to $b=2$ fm, a beam energy of 1 GeV/nucleon, using various nuclear mean fields, with and without Coulomb fields, and various reductions in the nucleon-nucleon cross section.

The effect of Δ resonances was also studied since the decay products receive an extra kick and this may be visible in the proton spectra. By tagging those protons whose last interaction before freezeout was a recoil from Δ decay and removing them from the BUU output, we were able to isolate their influence on the overall proton spectra. The results are presented below.

III. RESULTS

Our results for the impact-parameter-averaged calculations for 1 GeV/nucleon appear in Fig. 1. The temperature and radial flow velocities are consistent with those obtained in experiment [8] within uncertainties, and provides good evidence that BUU+coalescence is capable of reproducing this combination of radial and thermal motion in light fragments. Our simultaneous fit to the fragment spectra with a

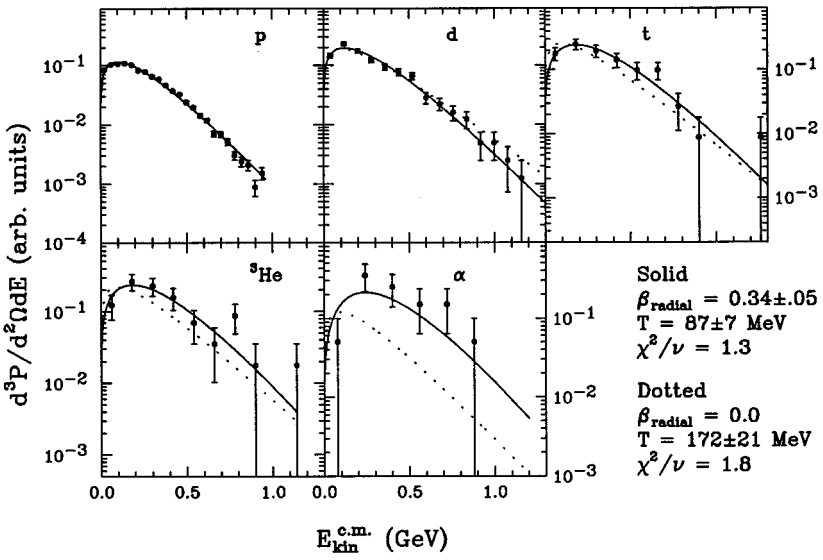

FIG. 1. Spectra of BUU plus coalescence for the impact-parameter-averaged Au + Au calculations at 1 GeV/nucleon and $\theta_{c.m.}=90°\pm15°$. Global temperature and radial flow velocity were obtained by fitting the radially expanding thermal model [15] to deuterons, tritons, ^{3}He, and alphas simultaneously. Dotted lines are the global fits for a radial flow velocity of zero.

nonzero radial flow velocity gave a minimum χ^2/ν of 1.3. Forcing a zero radial flow velocity yields a minimum χ^2/ν of 1.8, in keeping with, though not as dramatic as, the results of the EOS-TPC study [8]. Without absolute cross sections, normalizations were free parameters in our χ^2/ν minimization.

We extended our impact-parameter-averaged investigation to energies 250 MeV/nucleon, 600 MeV/nucleon, 1.5 GeV/nucleon, and 2 GeV/nucleon. The results are presented in Fig. 2. Here one can see that results from the calculations have significant overlap with experiment. Temperatures extracted from BUU+coalescence calculations agree well with those extracted from experiment, whereas our results for radial flow velocity agrees less well. They do suggest a saturation of radial flow velocity as beam energy is increased beyond 1 GeV/nucleon. Other models show a saturation at higher energies [41]. This is consistent with AGS data [42].

The microscopic features of our BUU transport code seem to have little influence on the radial flow velocity. We calculated the temperatures and radial flow velocities for reactions with an impact parameter of 2 fm and an energy of 1 GeV/nucleon. The results of the study are presented in Table II. Immediately, one can see the insensitivity of radial flow velocity to the equation of state and the in-medium modification of the nucleon-nucleon cross section. The nu-

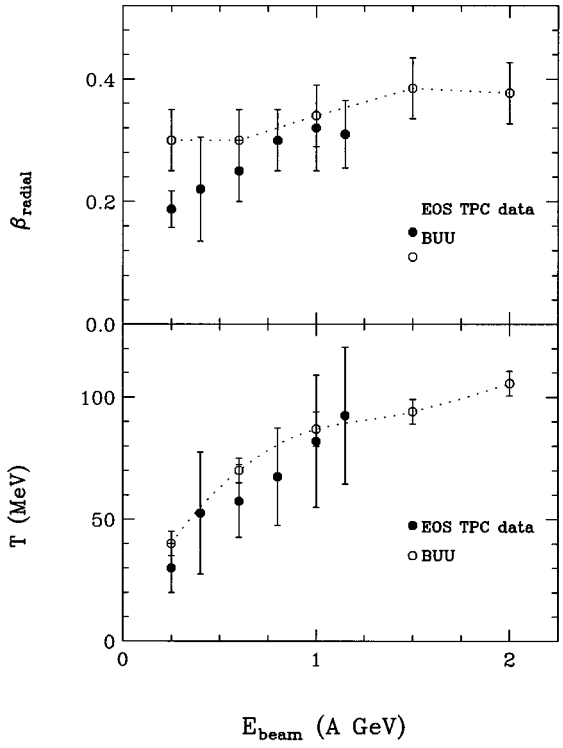

FIG. 2. Excitation function of radial flow velocity β and apparent temperature.

TABLE II. Effects of the microscopic features of BUU on apparent temperature and radial flow velocity.

EOS	$T\pm5$ (MeV)	$\beta\pm0.05$
	Coulomb, $\alpha=0$	
Stiff	70	0.35
Soft	80	0.35
Soft $\vec{p}$	75	0.35
Stiff $\vec{p}$	90	0.35
	No Coulomb, $\alpha=0$	
Stiff	70	0.35
Soft	70	0.30
Soft $\vec{p}$	95	0.35
Stiff $\vec{p}$	95	0.35
	Coulomb, $\alpha=-0.20$	
Stiff	75	0.35
Soft	65	0.35
Soft $\vec{p}$	80	0.35
Stiff $\vec{p}$	75	0.40
	Coulomb, $\alpha=-0.50$	
Stiff	70	0.35
Soft	65	0.35
Soft $\vec{p}$	70	0.35
Stiff $\vec{p}$	90	0.35

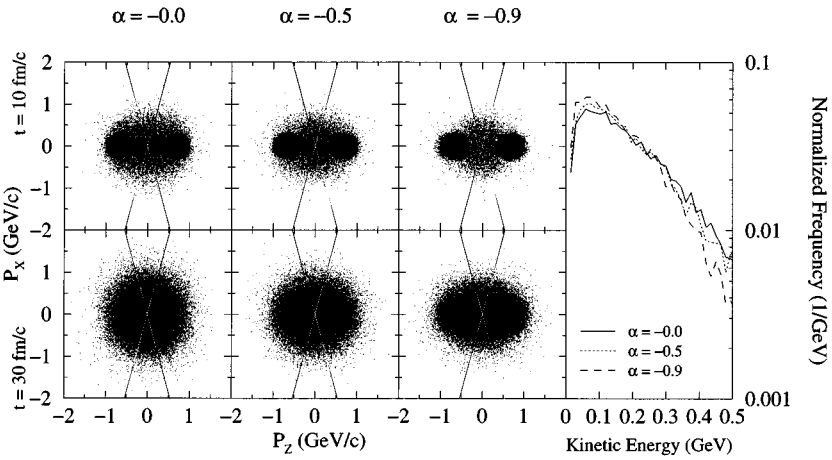

FIG. 3. The single-particle, reaction-plane momentum distributions for central Au on Au collisions using stiff, momentum-dependent mean field. α is the in-medium collision cross section reduction factor and the angular cuts are illustrated as black-white lines on the graphs. The rightmost panel is the kinetic energy distribution of the systems after 30 fm/c for various cross section reduction factors.

merical models used in the EOS-TPC study [8] also showed the radial flow velocity to have little dependence on the equation of state (EOS) used. Indeed, we cannot discern any significant EOS dependence. Radial flow will not develop within $\theta_{\text{c.m.}}=90°\pm15°$ of the beam axis without nucleon-nucleon collisions. For calculations at $b=2$ fm and $E_{\text{beam}}=1$ GeV/nucleon that were allowed to reach maximum compression before σ_{nn} was set to zero, almost no baryons obtained rapidities low enough to meet the kinematic selection criteria. However, we did see evidence that directed flow could be observed in those reactions. Thus we conclude that both nuclear mean fields and nucleon-nucleon collisions are important in the development of radial flow, and that it is likely that they provide roughly equal contributions to radial flow. We find that the magnitude of the radial flow, as opposed to the total radial kinetic energy, is chiefly governed by the beam energy.

In contrast, we do see striking changes in the unnormalized kinetic energy distributions of protons and light fragments as the mean fields and in-medium cross sections are changed. This is especially pronounced in the high energy tails of the light fragment spectra, with α's showing the most sensitivity. In addition, there is some sensitivity in the temperature of the light fragment spectra to momentum dependence in the nuclear mean field, as well as to the influence of the Coulomb field.

A. Temperature and microscopic features of BUU

There are some clear trends in the effects of the microscopic features of BUU on the extracted temperatures. The strongest is the addition of momentum dependence in the nuclear mean field. We see an increase in temperature as the momentum dependence is switched on in the calculations. The greatest increases are found in calculations devoid of Coulomb fields and using the free-space values of nucleon-nucleon cross sections. Smaller increases were found in those calculations which included the Coulomb fields.

The momentum-dependent terms in the mean field are repulsive at these energies. The addition of a repulsive mechanism should lead to lower densities and fewer collisions. One might expect this to decrease the extracted temperature. However, it seems that the repulsive momentum dependence tends to increase the amount of strongly thermalized matter splashing off of the hard, dense elliptical core that forms as maximum compression is reached. An explanation is that this matter, initially streaming in at beam velocity, is compressed and thermalized against this core. Since both density gradients (which by themselves offer some contribution via diffusive mechanisms) and momentum gradients are larger in the longitudinal directions than in the transverse directions, this matter will be ejected into the midrapidity regions. The ejection of this matter competes with the reduction of the collision rate to produce this result. This mechanism is sensitive to both the beam energy, which will set the relative importance of the mean field and collisions, and the impact parameter. Geometrical arguments imply that the angle of the major axis of this hard, dense core relative to the beam axis is strongly dependent upon the impact parameter.

There were weak trends with temperature variations and the reduction of the in-medium nucleon-nucleon cross section. We used the prescription of Eq. (2.2), where three values $\alpha=0,-0.2$, and -0.5 were taken. One might expect that as the collision cross section decreases, the amount of beam energy converted from directed and longitudinal to random and transverse kinetic energy decreases as well. This should manifest a lower temperature. Indeed, we found this to be true for those calculations using a soft momentum-dependent and the stiff momentum-independent mean fields. However, we found no discernible change when we used soft momentum-independent mean field, and found a slight increase in temperature while using the stiff momentum-dependent mean field.

The weakness of these trends is due to the dominant role the first few nucleon-nucleon collisions play in the final single-particle kinetic energy distributions. Figure 3 shows the single-particle momentum distributions for central Au on Au collisions at 1 GeV/nucleon and using 200 test particles per nucleon. The top row of graphs show the distributions early in the calculations, after 10 fm/c. Here the two Fermi spheres of the initial state are clearly seen. The clouds around the origin represent the nucleons elastically scattered in these early stages. The lower row of graphs are the distributions after 30 fm/c. The kinematic cuts are represented graphically as the black-white lines intersecting the origins. Within these cuts, one can see the initial collisions' strong influence on the intermediate- and high-energy portions of the kinetic energy distributions after 30 fm/c. As a result, the

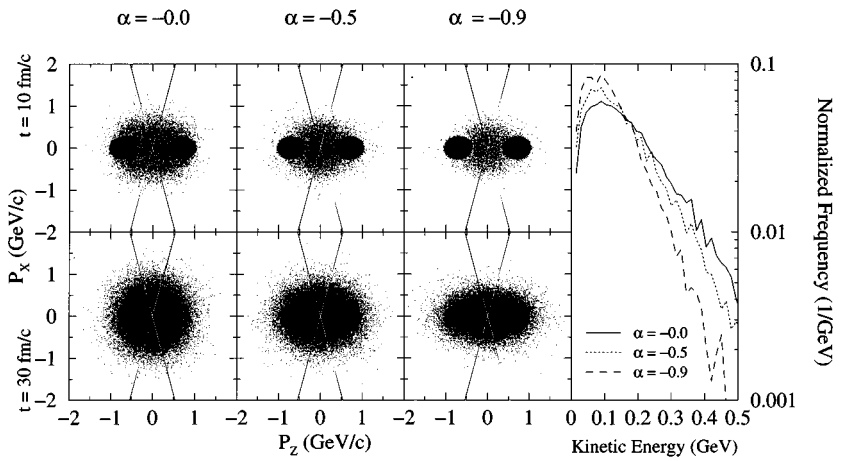

FIG. 4. Same as Fig. 3 except using soft, momentum-independent mean field.

temperature becomes sensitive to the kinematics of the initial state, namely the beam energy. The weakness of the sensitivity of the apparent temperature to the in-medium cross section is shown in the right-hand panel. Here the slopes, and thus the apparent temperature, of the kinetic energy distributions are similar.

Figure 4 shows the same information as Fig. 3, but for calculations using a soft, momentum-independent equation of state. As the figure shows, most of the intermediate- and high-energy portions of the final kinetic energy distributions are dominated by collisions occurring after 10 fm/c. These collisions are subject to in-medium effects, and as a result, temperature manifests a sensitivity to α. This sensitivity on α, however, is surprisingly small. This is because nucleons that scatter elastically to 90° are constrained by momentum and energy conservation. And to first order, these kinematic constraints are only sensitive to the beam energy. Thus, even if we drastically decrease the scattering probabilities, the nucleons that do scatter to 90° have similar slope parameters in their energy spectrum. The net result is that the slope parameters only show limited sensitivity to the magnitude of the in-medium cross section.

That this limited sensitivity does not materialize in the light-fragment spectra is due primarily to the imposition of our coalescence model on the single-particle phase-space distribution upon freeze out. Since we found the light fragment spectra to be relatively insensitive to the critical coalescence radii in configuration space while sensitive to the momentum-space radius, to first order the coalescence model used in this study is a momentum-space coalescence. Figure 4 shows that a momentum-space coalescence radius of 100 MeV/c is too large to adequately resolve the nucleon density gradient in momentum space. This effectively integrates out the features of momentum distribution that would likely lead to different global temperatures in the light-fragment spectra as the collision cross section is modified. However, this radius was found to most accurately reproduce the proton kinetic energy spectra from the EOS-TPC experiment [8].

Finally, to study the effects of Δ decays on the final-state proton spectra, we calculated the spectra with and without those protons coming from Δ decays. There was concern that the recoil protons receive from the decays would contaminate the spectra. Protons created in Δ decays as a final interaction, are unlikely to contain information about the radial flow and the temperature of the system that created the Δ's. In an effort to isolate this effect, we tagged those protons whose last interaction was a recoil from a Δ decay. We saw little change in the spectra when those recoiling protons were removed. This is somewhat contrary to what was reported by the EOS-TPC Collaboration [8].

IV. CONCLUDING REMARKS

A clear nonthermal component has been found in light-fragment spectra in Au + Au collisions at beam energies 0.25, 0.60, 1.0, 1.5, and 2.0 GeV/nucleon with the application of a coalescence model to phase-space output from the BUU transport equation. This hybrid model successfully reproduced the observed temperature and radial flow velocity, within estimated uncertainties, found in light fragment spectra in a recent experiment [8]. Furthermore, we find unfortunately that the radial flow velocity shows little sensitivity to the microscopic features of BUU.

The global temperature extracted from the final-state light-fragment spectra shows weak dependence on in-medium modifications of the nucleon collision cross section. Lower cross sections led to lower temperatures when used in conjunction with a soft, momentum-dependent mean field and a stiff, momentum-independent mean field. From our calculations of the single-particle momentum distributions of central Au on Au collisions at 1 GeV/nucleon using a stiff, momentum-dependent mean field, we find the final kinetic energy distributions to be dominated by beam kinematics. For calculations using a soft, momentum-independent mean field, we find the momentum-space coalescence radius to be too coarse to resolve the in-medium effects.

Protons from Δ decays were found to have little effect on the final-state proton spectra at 1 GeV/nucleon.

ACKNOWLEDGMENT

This work was supported in part by the National Science Foundation under Grant PHY-9403666 and NSF PFF Grant PHY-9253505.

[1] P. Danielewicz and G. Odyniec, Phys. Lett. **157B**, 146 (1985).
[2] G. F. Bertsch, W. G. Lynch, and M. B. Tsang, Phys. Lett. B **189**, 384 (1987).
[3] C. A. Ogilvie, D. A. Cebra, J. Clayton, P. Danielewicz, S. Howden, J. Karn, A. Nadasen, A. Vander Molen, G. D. Westfall, W. K. Wilson, and J. S. Winfield, Phys. Rev. C **40**, 2592 (1989).
[4] C. Gale, G. M. Welke, M. Prakash, S. J. Lee, and S. Das Gupta, Phys. Rev. C **41**, 1545 (1990).
[5] G. D. Westfall, C. A. Ogilvie, D. A. Cebra, W. K. Wilson, A. Vander Molen, W. Bauer, J. S. Winfield, D. Krofcheck, J. Karn, S. Howden, T. Li, R. Lacey, K. Tyson, and M. Cronqvist, Nucl. Phys. **A519**, 141 (1990).
[6] C. A. Ogilvie, W. Bauer, D. A. Cebra, J. Clayton, S. Howden, J. Karn, A. Nadasen, A. Vander Molen, G. D. Westfall, W. K. Wilson, and J. S. Winfield, Phys. Rev. C **42**, R10 (1990).
[7] G. D. Westfall, W. Bauer, D. Craig, M. Cronqvist, E. Gualtieri, S. Hannuschke, S. Klakow, T. Li, T. Reposeur, A. M. Vander Molen, W. K. Wilson, J. S. Winfield, J. Yee, S. J. Yenellow, R. Lacey, A. Elmaani, J. Lauret, A. Nadasen, and E. Norbeck, Phys. Rev. Lett. **71**, 1986 (1993).
[8] M. A. Lisa *et al*., Phys. Rev. Lett. **75**, 2662 (1995).
[9] G. M. Welke, M. Prakash, T. T. S. Kuo, S. Das Gupta, and C. Gale, Phys. Rev. C **38**, 2101 (1988).
[10] M. B. Tsang, G. F. Bertsch, W. G. Lynch, and M. Tohyama, Phys. Rev. C **40**, 1685 (1989).
[11] G. F. Bertsch, H. Kruse, and S. Das Gupta, Phys. Rev. C **29**, 673 (1984).
[12] J. Aichelin and G. F. Bertsch, Phys. Rev. C **31**, 1730, (1985).
[13] G. F. Bertsch and S. Das Gupta, Phys. Rep. **160**, 189 (1988).
[14] C. Gale, G. F. Bertsch, and S. Das Gupta, Phys. Rev. C **35**, 1666 (1987).
[15] P. J. Siemens and J. O. Rasmussen, Phys. Rev. Lett. **42**, 880 (1979).
[16] M. Lisa *et al.*, Phys. Rev. Lett. **75**, 2662 (1995).
[17] C. Gale *et al.*, Phys. Rev. C **41**, 1545 (1990).
[18] D. Klakow, G. Welke, and W. Bauer, Phys. Rev. C **48**, 1982 (1993).
[19] T. Alm, G. Röpke, W. Bauer, F. Daffin, and M. Schmidt, Nucl. Phys. **A587**, 815 (1995).
[20] J. L. Nagle, B. S. Kumar, D. Kusnezov, H. Sorge, and R. Mattiello, Phys. Rev. C **53**, 367 (1996).
[21] B. V. Jacak, D. Fox, and G. D. Westfall, Phys. Rev. C **31**, 704 (1984).
[22] H. Kruse, B. V. Jacak, J. J. Molitoris, G. D. Westfall, and H. Stöcker, Phys. Rev. C **31**, 1770 (1985).
[23] J. L. Nagle, B. S. Kumar, M. J. Bennett, S. D. Coe, G. E. Diebold, and J. K. Pope, Phys. Rev. Lett. **73**, 2417 (1994).
[24] S. T. Butler and C. A. Pearson, Phys. Rev. **129**, 836 (1963).
[25] A. Mekjian, Phys. Rev. Lett. **38**, 640 (1977).
[26] J. I. Kapusta, Phys. Rev. C **21**, 1301 (1980).
[27] S. Das Gupta and A. Z. Mekjian, Phys. Rep. **72**, 131 (1981).
[28] H. Sato and K. Yazaki, Phys. Lett. **98B**, 153 (1981).
[29] L. P. Csernai and J. I. Kapusta, Phys. Rep. **131**, 223 (1986).
[30] A. Schwarzchild and C. Zupančič, Phys. Rev. **129**, 854 (1963).
[31] J. Gosset, H. H. Gutbrod, W. G. Meyer, A. M. Poskanzer, A. Sandoval, R. Stock, and G. D. Westfall, Phys. Rev. C **16**, 629 (1977).
[32] M. C. Lemaire, S. Nagamiya, S. Schnetzer, H. Steiner, and I. Tanihata, Phys. Lett. **85B**, 38 (1979).
[33] M. B. Tsang, W. G. Lynch, R. Ronningen, A. Chen, C. K. Gelbke, T. K. Nayak, J. Pochodzalla, F. Zhu, M. Tohyama, W. Trautmann, and W. Dünnweber, Phys. Rev. Lett. **60**, 1479 (1988).
[34] S. Wang *et al.*, Phys. Rev. Lett. **74**, 2646 (1995).
[35] J. Barrette *et al*., Phys. Rev. C, **50**, 1077 (1994).
[36] H. Sorge, J. L. Nagle, and B. S. Kumar, Phys. Lett. B **355**, 27 (1995).
[37] C. B. Dover, U. Heinz, E. Schnedermann, and J. Zimányi, Phys. Rev. C **44**, 1636 (1991).
[38] W. J. Llope, S. E. Pratt, N. Frazier, R. Pak, D. Craig, E. E. Gualtieri, S. A. Hannuschke, N. T. B. Stone, A. M. Vander Molen, G. D. Westfall, J. Yee, R. A. Lacey, J. Laurent, A. C. Migerey, and D. E. Russ, Phys. Rev. C **52**, 2004 (1995).
[39] P. Danielewicz and G. F. Bertsch, Nucl. Phys. **A53**, 712 (1991).
[40] P. Danielewicz, Phys. Rev. C **51**, 716 (1995).
[41] B. A. Li, C. M. Ko, ''Excitation Functions in Central Au+Au Collisions,'' Texas A&M Report nucl-th/9601041.
[42] J. Harris, W. Lynch, B. Zajc, W. Bauer, M. Gyulassy, J. Natowitz, and J. Stachel, ''Intermediate and High Energy Heavy-Ion Reactions: NSAC/DNP Town Meeting,'' Brookhaven National Laboratory report 1995.